

A hybrid surrogate-assisted integrated optimization of horizontal well spacing and hydraulic fracture stage placement in naturally fractured shale gas reservoir



Lian Wang^{a, **}, Yuedong Yao^{a,*}, Guoxiang Zhao^a, Caspar Daniel Adenutsi^c, Wenzhi Wang^b, Fengpeng Lai^d

^a State Key Laboratory of Petroleum Resources and Prospecting, China University of Petroleum, Beijing, 102249, China

^b CNPC Engineering Technology R&D Company Limited, Beijing, 102206, China

^c Reservoir Simulation Laboratory, Department of Petroleum Engineering, Faculty of Civil and Geo-Engineering, Kwame Nkrumah University of Science and Technology, Kumasi, Ghana

^d School of Energy Resources, China University of Geosciences, Beijing, 100083, China

ARTICLE INFO

Keywords:

Shale gas reservoir
Horizontal well spacing
Fracture stage placement
Integrated optimization
Transfer stacking
Hybrid surrogate model

ABSTRACT

Horizontal well drilling and hydraulic fracturing are the most frequently adopted technologies for the commercial development of shale reservoirs. However, expensive production strategies are still implemented which results in high risk in investment. Integrated optimization of horizontal well spacing and hydraulic fracture stage placement helps in striking a balance between gas production and economic benefits. Previous studies relied heavily on numerical simulation models which are computationally expensive. In this study, a novel hybrid surrogate-assisted shale gas horizontal well spacing and hydraulic fracture stage placement multi-objective optimization method based on transfer stacking (SATS-WSF) is proposed to lessen the computational burden of the numerical simulation model run. In the SATS-WSF method, three widely used machine learning models, namely Gaussian process regression (GPR), radial basis function network (RBFN), and support vector regression (SVR) were applied to approximate the numerical simulation model as the source tasks. Then, a hybrid surrogate model transferring the three source tasks to the computationally expensive numerical simulation model was adopted to guide the optimization process of shale gas horizontal well spacing and hydraulic fracture stage placement. In addition, two sampling infill strategies called promising and uncertain were used to accelerate the searching process and to improve the quality of the final optimal solutions. Furthermore, two cases with different wells and fracture types based on the Barnett shale gas reservoir properties were employed to verify the effectiveness and efficiency of the SATS-WSF method. This method provides an intelligent approach for efficient decision-making of shale gas well space and fracture scheme.

1. Introduction

There has been a sharp increase in the demand for fossil energy resources, especially natural gas, in recent years due to industrialization and the development of human society (IEA, 2020). The efficient development of shale gas resources plays an essential role in ensuring natural gas supply. Field development practice and academic research during the past years have shown that horizontal well drilling and hydraulic fracturing technologies are the best methods to economically and efficiently develop shale gas resources (Waters et al., 2009; Clarkson

et al., 2012). Nevertheless, because of the sophisticated flow behavior and natural fracture distribution in ultralow porosity and permeability shale gas reservoirs, development of such reservoirs by horizontal well drilling and hydraulic fracturing technologies is usually accompanied by huge investment risks and high costs (Rahmanifard and Plaksina, 2018; Berawala and Andersen, 2019; Feng et al., 2018, 2021; Sherratt et al., 2021; Zhang et al., 2020, 2021; Zhang and Sheng, 2021). Thus, precisely and optimally designing well spacing and fracture stage placement of the hydraulic fractured wells in naturally fractured shale gas reservoirs is one of the most important challenges for efficient and economical

* Corresponding author.

** Corresponding author.

E-mail addresses: wanglian02@163.com (L. Wang), yaoqedong@163.com (Y. Yao).

development of shale gas resources (Yu and Sepehrnoori, 2013; Xu et al., 2018). Numerical simulation technique is often applied to characterize the flow mechanisms and multi-scale fractures in shale gas reservoirs. Also, most of the previous horizontal well spacing and fracture optimization design studies relied on numerical simulation models in order to evaluate the objectives (Jahandideh and Jafarpour., 2016; Zhang et al., 2019).

With regards to horizontal well spacing and fracture optimization design, scholars have extensively done a lot of related research work of certain and uncertain optimization. For certain optimization, Plaksina and Gildin (2017) applied the genetic algorithm (GA) for integrated optimization of fracture and well parameters. Based on GA and numerical simulation model, Moradi and Jamialahmady (2018) optimized some fracture related parameters of a fractured horizontal well. Zhang and Sheng (2020) considered stimulated reservoir volume (SRV) and modified the particle swarm optimization (PSO) algorithm for horizontal well fracturing of shale gas reservoirs without considering the natural fracture in the reservoir model. More recently, Yao et al. (2021) modified the PSO algorithm for dimension-varying fracturing parameters optimization of shale gas reservoir. These researches have achieved great success in the optimization of well spacing and fracture stage placement through making full use of the global search capability of nature-inspired algorithms such as GA and PSO. For uncertain optimization, the uncertainty of reservoirs can be considered as geological parameters such as porosity (Santoso et al., 2019), permeability (Omar et al., 2021), natural fracture distribution (Zhang and Sheng, 2021), and fracture characteristics (He et al., 2021; Santoso et al., 2021). Podhoretz and Valkó (2014) developed a methodology for making strategic decisions regarding the number and dimensions of hydraulic fractures. The methodology was then applied to the Lower Tertiary formation in the Gulf of Mexico. Baioco et al. (2019) considered the uncertainty of drainage radius, permeability, net-pay, temperature and pressure of the reservoir to simultaneously maximize the production of a fractured well and minimize the fracture cost. Zhang and Sheng (2021) considered geological uncertainty for the optimization of a hydraulically fractured well.

However, the tremendous computational burden of the expensive numerical simulation model runs during the iterative optimization process is inevitable. Therefore, these methods are time-consuming and unable to meet the requirement of fast decision-making of well spacing and fracture stage placement scheme in shale gas reservoirs. In summary, these optimization strategies are not adequate in terms of obtaining an optimization scheme in a short time and this significantly affects the development efficiency of shale gas reservoirs. With this challenge, it is important to establish precise and a fast shale gas well spacing and fracture stage placement optimization method.

A popular method to address this issue is surrogate-assisted strategy. This strategy applies simple-yet-precise models to replace the computationally expensive numerical simulation process. Due to convenience in their operation and flexible application, machine learning models such as artificial neural network (ANN), support vector regression (SVR), radial basis function (RBF), and Gaussian process regression (GPR) have shown great performances in well control parameters optimization (Guo and Reynolds, 2018; Chen et al., 2020; Wang et al., 2020, 2021; Jin et al., 2020), well placement optimization (Pouladi et al., 2017; Ding et al., 2020; Kim et al., 2021), fracturing parameters optimization (Zhang et al., 2019; Zhang and Sheng, 2021), and history matching (Aanonsen et al., 2019). Despite the application of the aforementioned machine learning algorithms, research on how to reduce the computational burden of the optimization iteration process of shale gas reservoir is far from enough. Meanwhile, the application of surrogate-assisted technique to integrated optimization design of horizontal well spacing and fracture stage placement in shale gas reservoir is scarce. Furthermore, most of the existing methods independently use a single surrogate model and neglect the potential synergies between these models.

With the experiences from reservoir production optimization (Desbordes et al., 2022; Zhang et al., 2022; Zhong et al., 2022), transfer learning is regarded as one of the most promising ways to make full use of the potential synergies of these existing single surrogate models. With that in mind, transfer stacking technique (Pan and Yang, 2009) which is one of the most popular transfer learning methods is adopted in this study to transfer knowledge from three single models (GPR, RBFN, and SVR) in establishing a hybrid surrogate model. During the process, the knowledge of the three models realizes efficient transfer and fully utilizes the potential synergies of the models. To this end, a hybrid surrogate-assisted method for horizontal well spacing and hydraulic fracture stage placement based on transfer stacking (SATS-WSF) is proposed so as to lessen the computational burden of expensive numerical simulation models. In the meantime, the evaluation error of the hybrid surrogate model is ineluctable and this may mislead the iteration process. To accelerate the convergence speed and improve the quality of the final optimization solutions, two infill sampling strategies namely “promising” and “uncertain” are adopted to infill samples and update the surrogate model during the iteration process.

The rest of this paper is organized as follows. In section 2, the integrated shale gas well spacing and fracture stage placement optimization model and its associated terminologies are introduced. The details of the proposed SATS-WSF and related strategies are presented in section 3. section 4 discussed the performance of the SATS-WSF method on two cases with different wells and fracture types in a naturally fractured shale gas reservoir. Finally, section 5 gives the conclusions of this research and lists the prospects for future work.

2. Integrated optimization model

In this section, the integrated horizontal well spacing and hydraulic fracture stage placement optimization model is presented including the optimization design variables and objective functions.

2.1. Optimization variables

For this integrated horizontal well spacing and hydraulic fracture stage placement optimization problem, the geological and reservoir parameters are constants. Therefore, well spacing, the fracture half-length, the number of fractures, the fracture spacing as well as the well length are considered as the optimization variables because these parameters directly affect the productivity of the well and the investment in drilling and fracturing. Therefore, the optimization design variables are summarized as follows:

$$\mathbf{u} = [W_s, L_f, N_f, F_s, L]^T \quad (1)$$

where: W_s represents the well spacing, (m); L_f represents the fracture half-length, (m); F_s represents the fracture spacing, (m); N_f represents the number of fractured sections; L represents the horizontal length of the well, (m).

2.2. Optimization objective functions

Optimization problems can be defined as finding the most suitable variables to make the objective reach the maximum or minimum value. The general mathematical form is as follows:

$$\bar{\mathbf{u}} = \text{argmax}_f(\mathbf{u}) \quad (2)$$

where: \mathbf{u} is the vector of optimization variables; $f(\mathbf{u})$ is the objective function; $\bar{\mathbf{u}}$ is the optimal value vector of optimization variables after the optimization iteration process.

In the majority of previous studies on horizontal well spacing and fracture stage placement optimization, scholars only focused on single objective in obtaining maximum cumulative gas production (CGP) or achieving maximum net present value (NPV) (Lin et al., 2017; Plaksina

and Gildin, 2017; Rahamanifard and Plaksina, 2018; Xu et al., 2018; Zhang et al., 2019). Whereas, merely pursuing maximum CGP will result in huge investment during the fracturing stimulation operation. Meanwhile, pursuing maximum NPV alone will result in significant financial benefits, but will fail to fully utilize the production potential of the shale gas reservoir as well as ensure an adequate supply of natural gas with time. The ultimate goal of this multi-objective integrated horizontal well spacing and hydraulic fracture stage placement optimization is to obtain the maximum production potential of the reservoir with maximum economic benefits. Consequently, the net present value (NPV) and cumulative gas production (CGP) are set as the objectives in this multi-objective optimization (MOO) model to represent the economic index and production index, respectively. The detailed mathematical formulae of the two objectives are as follows:

$$f_1(\mathbf{u}) = \sum_{n=1}^{N_t} \frac{\Delta t_n}{(1+b)^{\frac{t_n}{365}}} \left[\sum_{j=1}^P \left(r_g \cdot q_{g,j}^n(\mathbf{u}) - O_j \right) \right] - \sum_{j=1}^P \sum_{i=1}^{N_f} (f_{ij} \cdot c_f) - \sum_{j=1}^P (w_j \cdot c_w) \quad (3)$$

$$f_2(\mathbf{u}) = \sum_{n=1}^{N_t} \sum_{j=1}^P q_{g,j}^n(\mathbf{u}) \quad (4)$$

where f_1 and f_2 represent the two objectives NPV and CGP, respectively; \mathbf{u} represents a vector of the optimization variables; r_g represents the current price of natural gas, (USD/m³); b represents the annual discount rate; N_t represents the shale gas production time steps; t_n represents the n -th step; Δt_n represents the size of the n -th time step (days); P represents the number of wells; O_j represents the daily operation cost of j -th well, (USD/day); $q_{g,j}^n$ represents the shale gas production rates of the j -th well in the n -th time step (m³/day); N_f represents the number of fracture stages; w_j represents the length of j -th well; f_{ij} represents the length of the i -th fracture in the j -th well; c_f and c_w represent the spend of fracturing operation and drilling per meter (USD/m), respectively.

Based on the above discussion of optimization variables and objectives, the purpose of this integrated optimization model is to find the most suitable horizontal well spacing and fracture stage placement scheme to maximize the two objectives. Meanwhile, some constrain conditions must be considered to satisfy the actual production situation. This is implemented by setting the upper boundary and the lower boundary of the optimization variables. Thus, constrain conditions of the integrated shale gas horizontal well spacing and hydraulic fracture stage placement optimization model is defined as follows:

$$\max_{\mathbf{u}} \mathbf{F}(\mathbf{u}) = (f_1(\mathbf{u}), f_2(\mathbf{u})) \quad (5)$$

$$\text{s.t. } \begin{cases} lb \leq \mathbf{u} \leq ub \\ F_s \cdot (N_f - 1) < L \end{cases} \quad (6)$$

where lb and ub represent the lower and upper boundaries of optimization variables, respectively; F_s represents the space between fractures, (m); N_f represents the number of fractured sections; L represents the horizontal length of well, (m).

3. Related work

3.1. Framework of multi-task transfer stacking

Unlike the general machine learning methods, transfer learning fully utilizes the knowledge from source data (D_s) and source task (T_s) to guide the learning process of the target task (T_t) so as to enhance the evaluation accuracy of the T_t . Taking a regression problem as an example, the regression response of source task and target task are $S(\mathbf{x})$ and $T(\mathbf{x})$, and the source data D_s with p samples and target data D_t with m samples are expressed as $\{(x_1 s, y_1 s), \dots, (x_p s, y_p s)\}$ and $\{(x_1 t, y_1 t), \dots, (x_m t, y_m t)\}$. Ordinarily, the source task and the target task are not the same problems and the number of source data is greater than the target data.

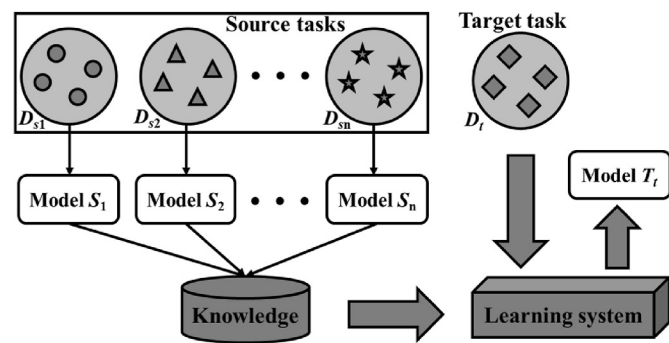


Fig. 1. Diagram of transfer stacking.

Transfer stacking strategy is one of the most commonly used transfer learning methods, which is suitable for regression problems (Pan and Yang, 2009). More specifically, Fig. 1 displays n data sources $D_{s1}, D_{s2}, \dots, D_{sn}$ training n regression models S_1, S_2, \dots, S_n , with transfer stacking combining these models to guide the learning process of the target model T_t . Based on the theory of transfer stacking (Pardoe and Stone, 2010), the mathematical form of T_t is as follows:

$$T_t(\mathbf{x}) = \sum_{i=1}^n \alpha_i S_i(\mathbf{x}) + \alpha_{n+1} \quad (7)$$

where $\alpha = \{\alpha_1, \alpha_2, \dots, \alpha_n\}$ are the weight vector of source tasks; S_i is the i th regression model of n regression models; α_{n+1} represents the bias. These parameters are calculated by searching minimum mean squared error of $T_t(\mathbf{x})$ as follows:

$$MSE(\alpha) = \frac{1}{m} \sum_{j=1}^m (T_t(\mathbf{x}_j) - y_j)^2 = \frac{1}{m} \sum_{j=1}^m \left(\sum_{i=1}^n \alpha_i S_i(\mathbf{x}_j) + \alpha_{n+1} - y_j \right)^2 \quad (8)$$

where S_i is the i th regression model of n regression models; $(x_j t, y_j t)$ is the j th individual of D_t .

In this proposed multi-task transfer stacking hybrid surrogate model, three single surrogate models namely, Gaussian process regression (GPR), radial basis function network (RBFN), and support vector regression (SVR) are applied to approach the computationally expensive shale gas numerical simulation model ($f_h(\mathbf{x})$) through transfer learning. In this way, the source tasks (GPR, RBFN, SVR) can supply a large number of source data to substitute the computationally expensive shale gas numerical simulation model ($f_h(\mathbf{x})$). Thus, the proposed hybrid surrogate-assisted model integrates horizontal well spacing and hydraulic fracture stage placement optimization problem and transforms it into a transfer learning problem as follows:

- **Source task 1:** search the optimal of the GPR model $\bar{f}_{GPR}(\mathbf{x})$, which is trained by the source data D_{GPR} to approach the $f_h(\mathbf{x})$.
- **Source task 2:** search the optimal of the RBFN model $\bar{f}_{RBFN}(\mathbf{x})$, which is trained by the source data D_{RBFN} to approach the $f_h(\mathbf{x})$.
- **Source task 3:** search the optimal of the SVR model $\bar{f}_{SVR}(\mathbf{x})$, which is trained by the source data D_{SVR} to approach the $f_h(\mathbf{x})$.
- **Target task:** search the optimal of the $\bar{f}_t(\mathbf{x})$, which is trained by the target data D_t to approach the $f_h(\mathbf{x})$.

It is obvious that three source tasks (GPR, RBFN, SVR) are computationally cheap and easily available but the target task (Shale gas numerical simulation model) is time-consuming and difficult to obtain. Nevertheless, the three source tasks and target task possess potential synergies of each other. The target task can be approximated by these

source tasks via the transfer stacking strategy (Discussed in Section 3.2). Hence, in this proposed SATS-WSF method, a novel hybrid surrogate model $\bar{f}_t(\mathbf{x})$ for integrating the horizontal well spacing and hydraulic fracture stage placement optimization process is established to replace the computationally expensive shale gas numerical simulation model.

3.2. Hybrid surrogate modeling for shale gas optimization using transfer stacking

From the above discussion, the key point of the target task ($f_h(\mathbf{x})$) is establishing a hybrid surrogate model to approximate shale gas numerical simulation model by transferring the knowledge and using the potential synergies of the three source tasks (GPR, RBFN, SVR) during the integration of the horizontal well spacing and hydraulic fracture stage placement optimization process. With regards to the three source tasks (GPR, RBFN, SVR), the first one is building the GPR model $\bar{f}_{GPR}(\mathbf{x})$ using sample set D_{GPR} to approximate $f_h(\mathbf{x})$; the second is building the RBFN model $\bar{f}_{RBFN}(\mathbf{x})$ via sample set D_{RBFN} to approximate $f_h(\mathbf{x})$; and the last source task is building the SVR model $\bar{f}_{SVR}(\mathbf{x})$ through sample set

Algorithm 1 Pseudo code of target data selection in each iteration.

Input: D_{GPR} , D_{RBFN} , and D_{SVR} are the source data, P_t is the current iteration horizontal well spacing and hydraulic fracture stage placement schemes, nn is the number of schemes in P_t .

- 1: Empty the target data D_t .
- 2: **for** $i = 1$ to nn **do**
- 3: Search the nearest scheme of $P_i(NP)$ in D_{GPR} , D_{RBFN} , and D_{SVR} .
- 4: **if** NP does not belong to D_t **then**
- 5: Add NP to D_t .
- 6: **end if**
- 7: **end for**

Output: D_t .

D_{SVR} to approximate $f_h(\mathbf{x})$. The specific theories and super parameters of GPR, RBFN, and SVR models can be referred to in already published researches (Ounpraseuth, 2008; Chen et al., 2020; Drucker et al., 1996).

During the integration of the horizontal well spacing and hydraulic fracture stage placement optimization process, the transfer stacking strategy is conducted to improve the objectives evaluation accuracy for the horizontal well spacing and hydraulic fracture stage placement scheme of the hybrid surrogate model. Thus, the target data D_t is selected from the source data sets (D_{GPR} , D_{RBFN} , D_{SVR}) in each iteration step. The target data D_t , the hybrid surrogate model $\bar{f}_t(\mathbf{x})$ is used to substitute shale gas numerical simulation model transfers from the three source models ($\bar{f}_{GPR}(\mathbf{x})$, $\bar{f}_{RBFN}(\mathbf{x})$, and $\bar{f}_{SVR}(\mathbf{x})$) as follows:

$$\bar{f}_t(\mathbf{x}) = \alpha_1 \bar{f}_{GPR}(\mathbf{x}) + \alpha_2 \bar{f}_{RBFN}(\mathbf{x}) + \alpha_3 \bar{f}_{SVR}(\mathbf{x}) \quad (9)$$

where $\alpha = \{\alpha_1, \alpha_2, \alpha_3\}$ are the weight vector of three source tasks.

Obviously, equation (9) is different from the general equation form of transfer stacking as presented in equation (7). This is because with the iteration, the hybrid surrogate model is highly correlated to α_{n+1} in equation (7) and may mislead the optimization process. In that case, the bias (α_{n+1}) in equation (7) is discarded to reduce human interference of the integrated horizontal well spacing and hydraulic fracture stage placement optimization. Meanwhile, selection of the target data D_t directly affects the quality of the hybrid surrogate model. Thus, the data points in D_{GPR} , D_{RBFN} , and D_{SVR} which are close to any horizontal well spacing and hydraulic fracture stage placement scheme in the current

iteration schemes P_t are selected as the target data D_t . Therefore, the data in D_t is the neighbor of P_t so as to guarantee the evaluation accuracy of the hybrid surrogate model to P_t . The detailed procedures of target data D_t selection are displayed in **Algorithm 1**. Furthermore, the means of obtaining the weight vector $\alpha = \{\alpha_1, \alpha_2, \alpha_3\}$ plays an important role in modeling the hybrid surrogate model. The least square method was applied to determine the weight vector through searching the minimum mean squared error of $\bar{f}_t(\mathbf{x})$ for the current D_t , as displayed in equation (10).

$$MSE(\alpha_1, \alpha_2, \alpha_3) = \frac{1}{m} \sum_{j=1}^m (\alpha_1 \bar{f}_{GPR}(\mathbf{x}_t^j) + \alpha_2 \bar{f}_{RBFN}(\mathbf{x}_t^j) + \alpha_3 \bar{f}_{SVR}(\mathbf{x}_t^j) - y_t^j)^2 \quad (10)$$

To this end, the hybrid surrogate model $\bar{f}_t(\mathbf{x})$ achieves the property of adaptively improving its evaluation accuracy in integrating horizontal well spacing and hydraulic fracture stage placement optimization process.

Algorithm 1. Pseudo code of target data selection in each iteration.

3.3. The infill sampling strategy

There are inevitable errors in any surrogate assisted model optimization method. The proposed hybrid surrogate assisted model optimization method is no exception. These errors may interfere with the integrated horizontal well spacing and hydraulic fracture stage placement optimization process and unsatisfactory horizontal well spacing and hydraulic fracture stage placement schemes would be obtained. Thus, infilling a small number of new samples to the source data is one way to enhance the quality of the proposed hybrid surrogate model. Infilling some “promising” samples can improve the evaluation accuracy of the hybrid surrogate model in each iteration, while “uncertain” samples can enhance the distribution of the samples in the variables searching space (Tian et al., 2018). The above two sample infilling strategies accelerate the convergence of the optimization process and improve the dispersion of the final optimal solutions, respectively. When the hybrid surrogate model is established, the number of promising samples (\mathbf{x}_p) and uncertain samples (\mathbf{x}_u) which are equal to the objectives are evaluated by the numerical simulation model and infilled into D_{GPR} , D_{RBFN} , and D_{SVR} in each iteration step. The specific formula of the selection criterion is as follows:

$$\mathbf{x}_p = \underset{\mathbf{x} \in P_t \setminus D_{s1}, D_{s2}, D_{s3}}{\operatorname{argmax}} \bar{f}_t(\mathbf{x}) \quad (11)$$

$$\mathbf{x}_u = \underset{\mathbf{x} \in P_t \setminus D_{s1}, D_{s2}, D_{s3}}{\operatorname{argmax}} (|\bar{f}_{GPR}(\mathbf{x}) - \bar{f}_{RBFN}(\mathbf{x})| + |\bar{f}_{RBFN}(\mathbf{x}) - \bar{f}_{SVR}(\mathbf{x})| + |\bar{f}_{SVR}(\mathbf{x}) - \bar{f}_{GPR}(\mathbf{x})|) \quad (12)$$

In order to avoid repeated expensive shale gas numerical simulation runs, the promising and uncertain samples are chosen inside $P_t \setminus D_{GPR}$, D_{RBFN} , and D_{SVR} and added to D_{GPR} , D_{RBFN} , and D_{SVR} . The schemes with at least the largest objective value are selected as the promising samples, while the uncertain scheme \mathbf{x}_u are the individuals which have the largest objective value difference between the three source tasks. In this way, the GPR, RBFN, and SVR models as well as the hybrid surrogate model remodel at the start of each iteration of the integrated horizontal well spacing and hydraulic fracture stage placement optimization process.

3.4. Workflow of the SATS-WSF

This hybrid surrogate-assisted shale gas horizontal well spacing and hydraulic fracture stage placement optimization method contains three key sections: data, surrogate model, and optimization algorithm. Fig. 2 displays the detailed workflow of the SATS-WSF method. More specifically, the key point of the SATS-WSF method is establishing the hybrid surrogate model through transfer stacking. Three single surrogate models are built using the data sets generated by the Latin Hypercube Sampling (LHS) which is then evaluated by the shale gas numerical simulation model. Then, the transfer stacking strategy is applied to establish the hybrid surrogate model for replacing the shale gas numerical simulation model so as to evaluate the objectives. Furthermore, the main process of the SATS-WSF method is integrating horizontal well spacing and hydraulic fracture stage placement multi-objective optimization. Meanwhile, the non-dominated sorting genetic algorithm-II (NSGA-II) which is one of the most classical and computationally efficient multi-objective algorithms is applied as the optimizer (Deb et al., 2002). Therefore, the uniqueness of this SATS-WSF method is the hybrid surrogate model based on transfer stacking strategy which makes full use of the potential synergies of three single surrogate models. Besides, the infill sampling strategy is used to add promising and uncertain samples to source data for enhancing the quality of the hybrid surrogate model. The pseudo codes of the SATS-WSF method are shown in Algorithm 2.

Algorithm 2. pseudo code of SATS-WSF.

Algorithm 2: pseudo code of SATS-WSF

Input: Integrated well spacing and hydraulic fracture stage placement optimization problem with three source tasks ($\bar{f}_{GPR}(\mathbf{x})$, $\bar{f}_{RBFN}(\mathbf{x})$, $\bar{f}_{SVR}(\mathbf{x})$) and target task ($\bar{f}_t(\mathbf{x})$).
 1: Initial horizontal well spacing and hydraulic fracture stage placement scheme set P_0 with N schemes using Latin hypercube sampling (LHS).
 2: Evaluate the schemes in P_0 using shale gas numerical simulation model ($f_h(\mathbf{x})$) and build D_{GPR} , D_{RBFN} , and D_{SVR} with the n samples.
 3: Set $t = 1$.
 4: **while** the stop criteria are not met **do**
 5: Generate offspring scheme set Q_t using the scheme set P_{t-1}
 6: Establish $\bar{f}_{GPR}(\mathbf{x})$, $\bar{f}_{RBFN}(\mathbf{x})$, and $\bar{f}_{SVR}(\mathbf{x})$ using D_{GPR} , D_{RBFN} , and D_{SVR} , respectively.
 7: Select D_t from D_{GPR} , D_{RBFN} , and D_{SVR} using Algorithm 1.
 8: Establish the hybrid surrogate model $\bar{f}_t(\mathbf{x})$ from $\bar{f}_{GPR}(\mathbf{x})$, $\bar{f}_{RBFN}(\mathbf{x})$, and $\bar{f}_{SVR}(\mathbf{x})$ using D_t .
 9: Evaluate Q_t using $\bar{f}_t(\mathbf{x})$.
 10: Combine Q_t and P_{t-1} as P_t .
 11: Select N top schemes in P_t for next iteration.
 12: Infill the \mathbf{x}_p and \mathbf{x}^u schemes in D_{GPR} , D_{RBFN} , and D_{SVR} .
 13: $t = t + 1$.
 14: **end**
Output: the final optimal schemes.

4. Case study

In this part, the efficiency and accuracy of the SATS-WSF horizontal

well spacing and hydraulic fracture stage placement optimization method was verified by two cases with different wells and fracture stage placement types in shale gas reservoirs. Meanwhile, four traditional methods were chosen to demonstrate the performance of the SATS-WSF method. The four methods employed in the comparison are the Gaussian process regression model assisted optimization method (GPR-WSF), radial basis function network model assisted optimization method (RBFN-WSF), support vector regression model assisted optimization method (SVR-WSF), and numerical simulation model-based optimization method (NS-WSF). In addition, both the surrogate model and optimization algorithm will have some stochastic processes in their execution. Thus, twenty independent runs were adopted for each method in all cases to eliminate accidental error in the optimization. It is worth mentioning that the numerical simulation models for sampling and validation were run on the MATLAB Reservoir Simulation Toolbox (MRST) platform (Lie, 2019).

4.1. Case one: single well optimization

In this single well case, the SATS-WSF method is applied to a horizontal well spacing and hydraulic fracture stage placement integrated optimization problem in a homogeneous rectangular reservoir with natural fractures. The basic geological parameters of the Barnett shale were used in this reservoir model and the specific values of the main parameters are displayed in Table 1. The scale of this reservoir model is 1200 m × 300 m with the thickness of 20 m. Besides, the gas properties, transport and storage mechanisms, as well as geo-mechanic effects can be found in Wang (2020). The embedded discrete fracture model (EDFM) was applied to characterize the natural and hydraulic fractures in the numerical simulation model and this was realized by the HFM modules in the MRST (Lie, 2019). In order to make the reservoir model look real to the actual situation, the distribution of the natural fracture was referred to from Cao et al. (2016). The geometric diagram of this single well spacing and fracture stage placement optimization is displayed in Fig. 3. For the sake of reducing the impact of uncertainty, the horizontal well is drilled in the middle of the reservoir while the half-length and spacing of each fracture are the same. We assumed that the distribution of the hydraulic fractures extends from the middle of the well to either end.

The production schedule of this case is set as ten years with constant bottom hole pressure (BHP) of 3.5 MPa. Besides, the reservoir has closed boundary. Considering the actual size of the shale gas reservoir, the

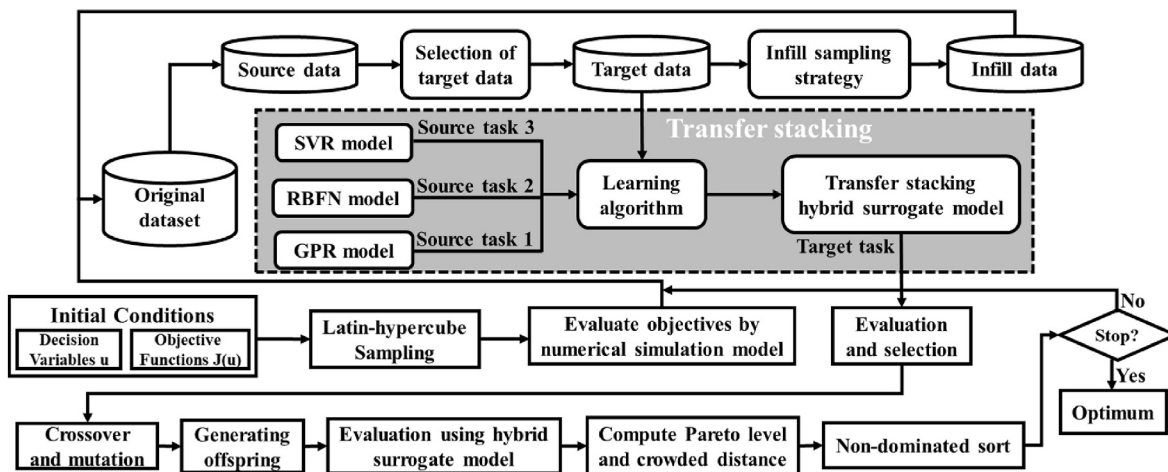


Fig. 2. Workflow of SATS-WSF.

Table 1
Reservoir parameters of this case.

Parameters	Value	Parameters	Value
Reservoir initial pressure	20.34 MPa	Langmuir pressure	4.47 MPa
Reservoir permeability	10^{-4} mD	Langmuir volume	2.72×10^{-3} m ³ /kg
Reservoir porosity	0.03	Gas viscosity	0.02 mPa s
Reservoir compressibility	4.4×10^{-4} MPa	Gas critical temperature	191 K
Hydraulic fracture conductivity	100mD*m	Gas critical pressure	4.64 MPa
Reservoir temperature	352 K	Gas molecular weight	16.04 $\times 10^{-3}$ kg/mol
Natural fracture porosity	0.3	Natural fracture permeability	0.01mD
Maximum principal stress	34 MPa	Minimum principal stress	29 MPa

search spaces of optimization design variable are shown in Table 2. Meanwhile, the economic parameters metrics for calculating the NPV are displayed in Table 3. The detailed parameters of the optimization algorithm used in this case are listed in Table 4.

In this case, the dimension of the optimization variables is four. Considering the dimension of the optimization variables and referring to previous researches (Zhang and Sheng, 2021), the LHS method was applied to generate three data sets (D_{GPR} , D_{RBFN} , and D_{SVR}) with 100 initial samples each in the searching space of optimization variables. These data sets were then evaluated by the numerical simulation model as the source data to train the GPR, RBFN, and SVR models for the GPR-WSF, RBFN-WSF, and SVR-WSF methods, respectively. With regards to the hybrid surrogate (HS) model, the target data were chosen from three source data sets (D_{GPR} , D_{RBFN} , and D_{SVR}) based on Algorithm

1. The HS model was then established by transfer stacking of the three single surrogate models. In this way, the initial samples for the HS model and the three single surrogate methods are the same in that the influence of initial conditions is controlled to the greatest extent. The mere differences between the HS model and the three single models are transfer stacking and infill sampling strategies. To validate the accuracy of the surrogate models, the initial samples were used for training while additional twenty samples generated by the LHS method were used for verification. The accuracy of the surrogate models was evaluated by the R^2 method (Omar et al., 2021). Figs. 4 and 5 show the surrogate models verification for the two objectives: NPV and CGP, respectively. These surrogate models were accurate enough and met the requirements of error accuracy, with R^2 values above 0.95.

One of the typical Pareto fronts (PFs) in the twenty independent runs

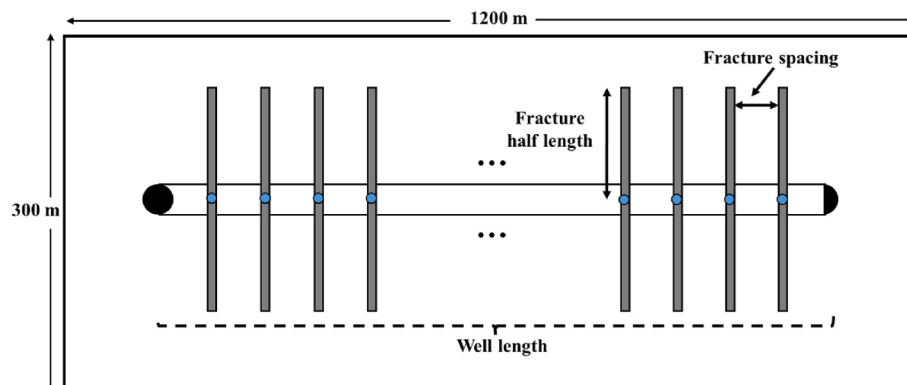


Fig. 3. Diagram of the single well optimization problem.

Table 2
Searching space of optimization variables.

Parameters	Symbol	Search space
Fracture spacing	r_g	[10, 70] m
Fracture half length	L_f	[0, 150] m
Well spacing	c_f	[100, 1000] m
Number of fractures	N_f	[1, 30]

Table 3
Parameters for NPV computation.

Parameters	Symbol	Value
Gas revenue	r_g	\$1/m ³
Cost of well drilling	c_w	\$2000/m
Cost of fracturing	c_f	\$500/m
Annual discount rate	D	0.05

Table 4
Relevant parameters of algorithms.

Parameter	Values
Size of population	50
Iterations	100
Mutative probability	0.005
Cross probability	0.65

of the five methods are shown in Fig. 6. As shown in Fig. 6, the PF of the SATS-WSF method had similar convergence and diversity with that of the NS-WSF method. This phenomenon qualitatively indicated that the SATS-WSF method obtained comparable results with the NS-WSF method. Conversely, the PF of the GPR-WSF, RBFN-WSF, and SVR-WSF methods performed worse than the other methods. Although the computational burden of the single surrogate model was negligible,

using only this model for horizontal well spacing and hydraulic fracture stage placement optimization will lead to inferior solutions. The potential synergies of the single surrogate models significantly improved the reliability and accuracy of the hybrid surrogate model due to the transfer stacking technique and sample infilling strategies.

To quantitatively evaluate the performance of the PFs obtained from these methods, two quality metrics called relative hyperarea difference (RHD) and overall spread (OS) were applied to measure the convergence and diversity of the PFs. The detailed formulas and definitions of RHD and OS can refer to Wang et al. (2022). It must be noted that the p_{good} and p_{bad} of this case were set as $[2.7 \times 10^6, 8.25 \times 10^6]$ and $[1.7 \times 10^6, 6.8 \times 10^6]$, respectively. The statistical parameters of RHD and OS for the five methods with twenty experiments are shown in Figs. 7 and 8. The mean values (MV) of RHD and OS for the SATS-WSF method were similar to those of the NS-WSF method. In this way, the optimal solutions obtained by SATS-WSF method had high quality. Conversely, the MV of RHD and OS of the other three single surrogate methods were worse than those of the SATS-WSF method. Meanwhile, the standard deviation (STD) of the SATS-WSF was smaller than the other three single surrogate methods. This shows the robustness of this transfer hybrid surrogate model. With regards to the computational cost, the number of simulation runs of the SATS-WSF method was about 500 times. This was about ten times less than that of the NS-WSF method which had about 5000 times HF model runs. Therefore, the transfer stacking technique and sample infilling strategy significantly improved the performance of the surrogate-assisted optimization method and reduced the computational burden of the numerical simulation-based evaluation process simultaneously.

After verifying and comparing the five methods, two representative solutions from the PF of the STSA-WSF method with maximum NPV and CGP were chosen as schemes one and two to better reveal the difference between the optimal solutions. The values of the optimization variables in the typical steps for scheme one are shown in Table 5, while that of

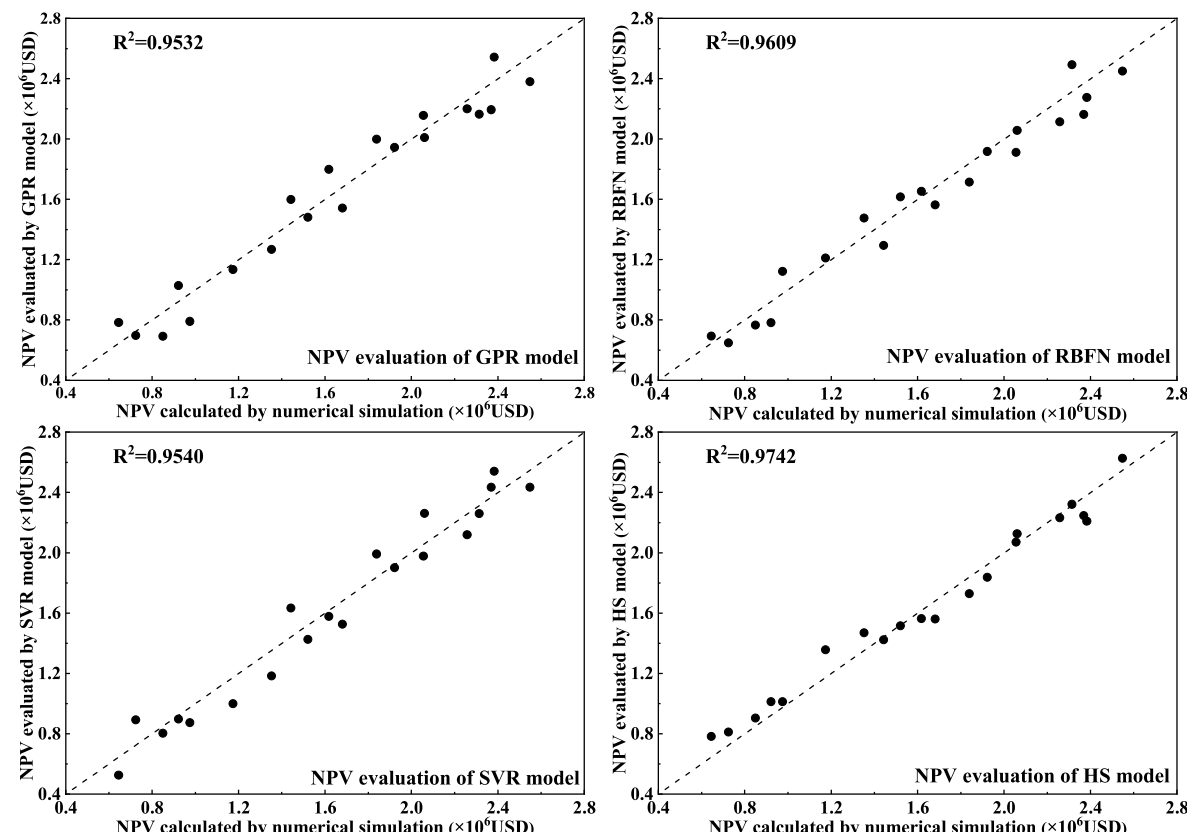


Fig. 4. Validation of the surrogate models for NPV.

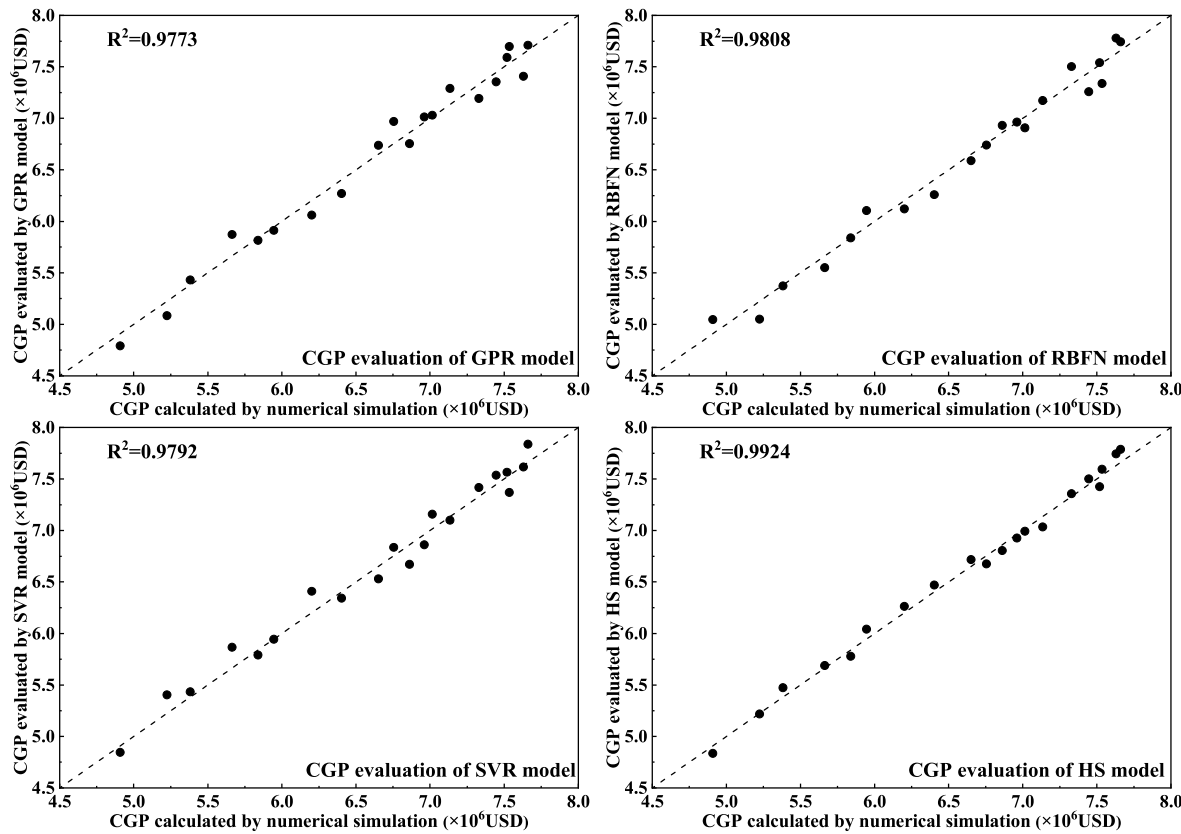


Fig. 5. Validation of the surrogate models for CGP.

scheme two are shown in Table 6. Furthermore, the pressure field after 10 years' production of the two schemes are shown in Fig. 9 and the NPV and CGP curves are depicted in Fig. 10. Using the optimized variables in scheme one, the maximum NPV can be obtained with relatively little investment and stimulation scale. Alternatively, the optimal variables in scheme two can obtain maximum gas production with huge investment and large-scale fracturing operation. Comparing the results of the two schemes, it was realized that all the objectives were unable to obtain the minimum or maximum values at the same time. This well matched the property of multi-objective optimization. Thus, field engineers can choose any solution in the PF as the best scheme according to the current

specific requirements. These results well demonstrated the superior performance of the SATS-WSF method on a single shale gas well optimization.

4.2. Case two: multi-well optimization

During the process of actual shale gas development, it is a common practice to drill multiple wells (multi-wells) from one platform. This is achieved the so-called "well factory" development. Thus, drilling multi-wells in one reservoir is adopted in this case to test and validate the SATS-WSF method. For the sake of simplicity, the shale gas reservoir and geological and engineering parameters in this case are the same as that

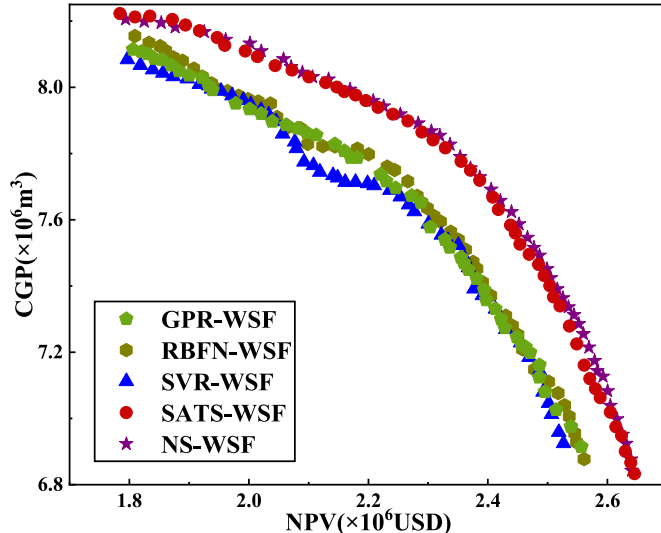


Fig. 6. Pareto fronts of different methods for case one.

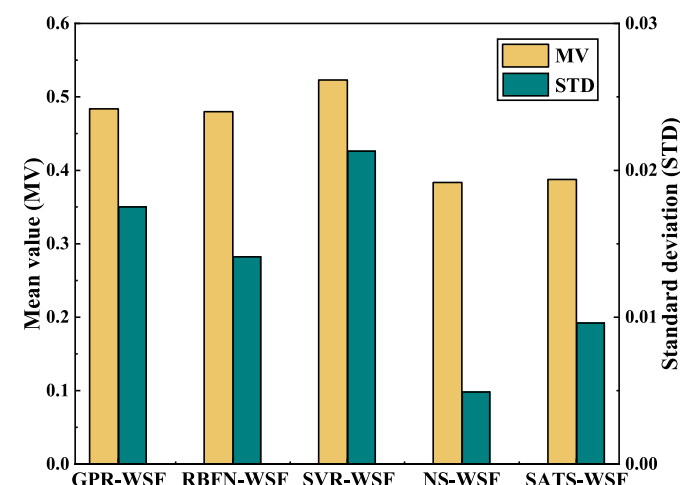


Fig. 7. The mean value (MV) and standard deviation (STD) of RHD obtained by the five methods for case one with twenty runs.

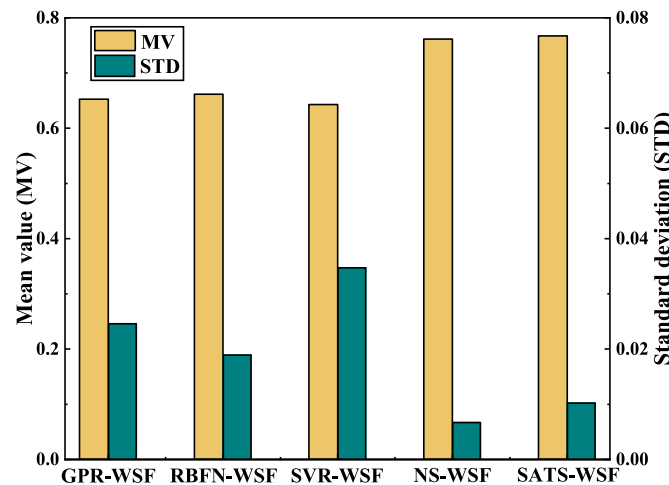


Fig. 8. The mean value (MV) and standard deviation (STD) of OS obtained by the five methods for case one with twenty runs.

of case one. Considering the size of the reservoir and actual well and fracture parameters, two wells are optimized simultaneously in this case. In addition, two types of fracture relationships, namely aligning and alternating fractures (Zhang and Sheng (2020)) are applied as types

1 and 2, respectively. The geometric diagrams of the two fracture types are displayed in Fig. 11. The constraint condition of type 1 is that the well spacing is greater than twice the fracture half-length, while type 2 has a well spacing that is greater than the fracture half-length.

The economic parameters as well as the parameters for the algorithm are the same as in case one and can be found in Tables 3 and 4. The well length, well spacing, fracture space, fracture half-length, and number of fractures are set as the optimization design variables and their search spaces are displayed in Table 7.

Just as in case one, the LHS method was once again used to generate three data sets with 100 initial samples each. These initial samples were subsequently evaluated by the numerical simulation model as the source data to train the GPR, RBFN, and SVR models for the GPR-WSF, RBFN-WSF, and SVR-WSF methods, respectively. With regards to the hybrid surrogate model, the target data were selected from the source data according to Algorithm 1. The hybrid surrogate model was established by transfer stacking of the three single surrogate models. It must be noted that the initial individuals of all the methods were also generated by the LHS method.

After optimization, one of the most representative PFs of the five methods in the twenty independent tests for the aligning and alternating fracture types are displayed in Figs. 12 and 13, respectively. It is seen that the PF of the SATS-WSF method had similar convergence and diversity with that of the NS-WSF method. It is worth mentioning that the

Table 5
Values of optimization variables in typical steps for scheme one with maximum NPV.

Optimization variables	Vales in step 1	Vales in step 25	Vales in step 50	Vales in step 75	Vales in step 100
Fracture space (m)	59.32	51.64	48.76	49.41	61.54
Fracture half-length (m)	74.98	83.43	101.32	118.36	125.27
Well length (m)	782.07	751.24	1124.13	962.31	992.52
Number of fractures	14	16	24	19	17

Table 6
Values of optimization variables in typical steps for scheme two with maximum CGP.

Optimization variables	Vales in step 1	Vales in step 25	Vales in step 50	Vales in step 75	Vales in step 100
Fracture space (m)	50.84	47.52	41.56	37.24	34.23
Fracture half-length (m)	81.27	98.53	117.89	125.32	133.85
Well length (m)	783.61	1037.24	1046.72	1025.48	1013.78
Number of fractures	16	22	26	28	30

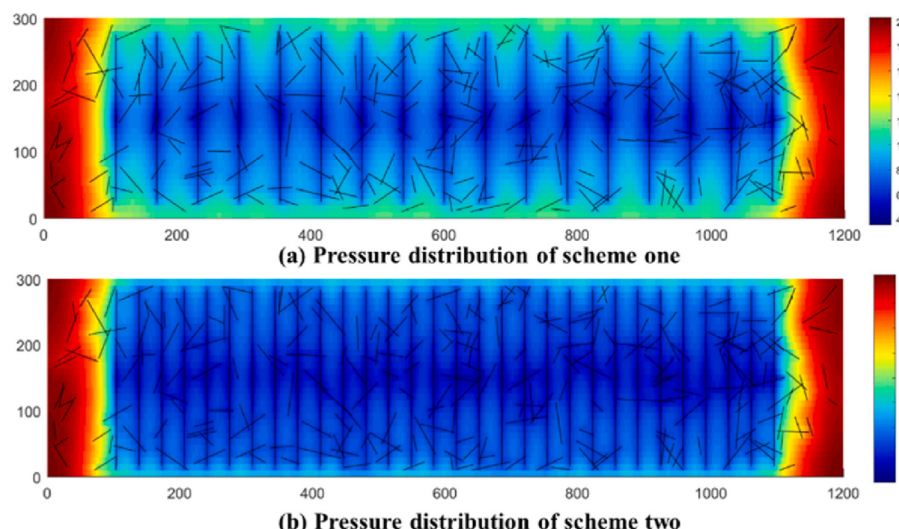


Fig. 9. Pressure distributions of two schemes after 10 years' production in case one (MPa).

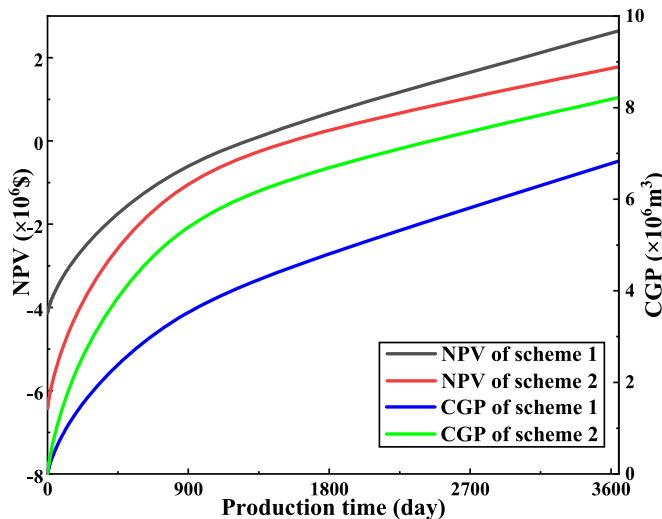


Fig. 10. NPV and CGP curves of scheme 1 and 2 in case one.

objective values of the type 2 were larger than that of type 1. Therefore, type 2 can obtain more economic benefits and gas production than type 1, and it is more suitable for shale gas “well factory” development. By contrast, the PFs of the GPR-WSF, RBFN-WSF, and SVR-WSF methods were dominated by the SATS-WSF and NS-WSF methods. Consequently, only relying on the single surrogate model for objective evaluation will lead to inferior solutions. These phenomena intuitively demonstrated the better performance of the SATS-WSF method in this multi-well optimization case.

Subsequently, the quantitative analysis of the convergence and diversity of the PFs in these methods were also assessed by RHD and OS, respectively. The two endpoints p_{good} and p_{bad} were set as $[2.7 \times 10^6, 10.5 \times 10^6]$ and $[1.8 \times 10^6, 8.8 \times 10^6]$ for type 1 and as $[3.4 \times 10^6, 11 \times 10^6]$ and $[2.1 \times 10^6, 9.5 \times 10^6]$ for type 2 in this case. The statistical parameters of RHD and OS with twenty runs of the two fracture types are shown in Figs. 14 and 15, respectively. The RHD and OS values of the SATS-WSF method were better than the three single surrogate methods but equivalent to that of the NS-WSF method. Hence, the PFs obtained from the SATS-WSF method were of high quality, accurate and reliable in both fracture types. With regards to the computational burden, the SATS-WSF method was about twenty-five times less than that of the NS-WSF method. This lessened the computational cost of the numerical simulation model for objective evaluation significantly. The above quantitative description verified the superior performance of the SATS-WSF method with respect to convergence, diversity, and computational efficiency.

To further analyze and better understand the solutions obtained by the SATS-WSF method, solutions with maximum NPV and CGP in both

fracture types were chosen as schemes one and two. The design variables in typical steps for schemes one and two of type 1 are listed in Tables 8 and 9, while for these of type 2 are shown in Tables 10 and 11. Subsequently, the pressure fields for the two schemes of the two fracture types after ten years’ production are displayed in Figs. 16 and 17. Furthermore, the NPV and CGP curves for two schemes of the two fracture types are shown in Fig. 18. It is seen that the NPV and CGP curves of type 2 were higher than that of type 1. In this way, the alternating fracture type is more suitable for multi-well development and this fracture type can obtain better economic value and gas production than aligning fracture type.

5. Conclusion

In this study, a novel integrated horizontal well spacing and hydraulic fracture stage placement multi-objective optimization method based on hybrid surrogate model with transfer stacking technique

Table 7
Searching space of optimization variables.

Parameters	Symbol	Search space
Fracture spacing	F_s	$[10, 70] \text{ m}$
Fracture half-length	L_f	$[0, 75] \text{ m}$
Well length	L	$[100, 1200] \text{ m}$
Number of fractures	N_f	$[1, 30]$
Well spacing	W_s	$[10, 150] \text{ m}$

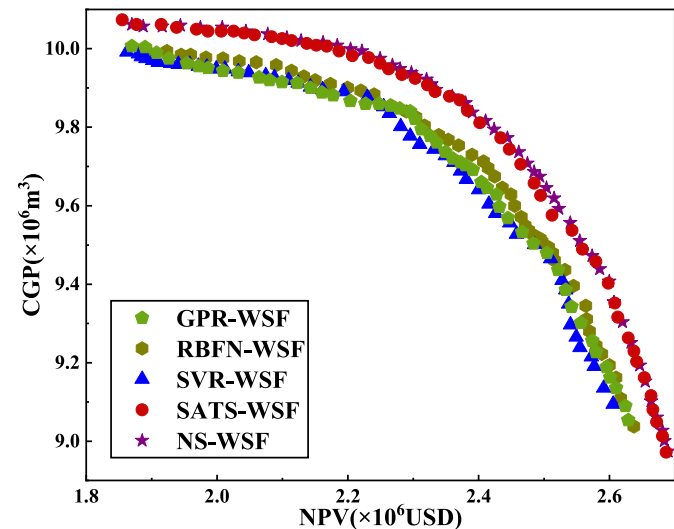


Fig. 12. Pareto fronts of different methods for type 1.

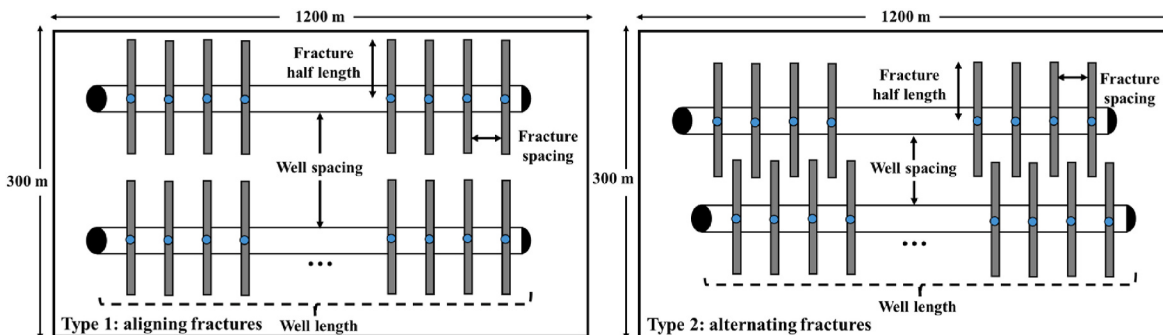


Fig. 11. Diagram of the two types of fracture relationship.

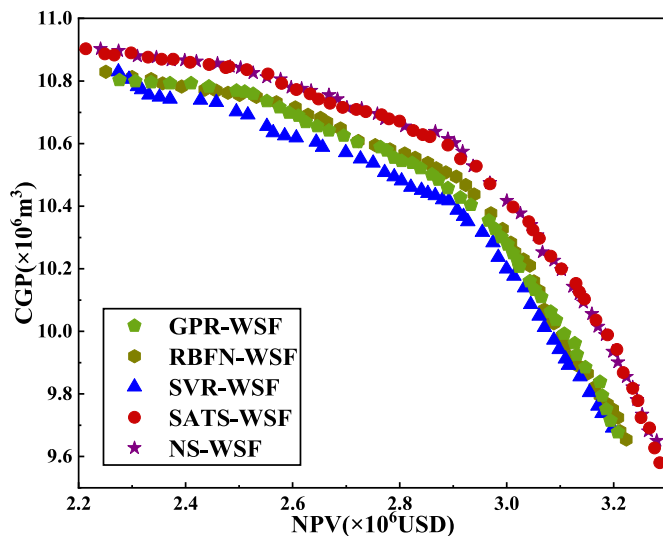


Fig. 13. Pareto fronts of different methods for type 2.

(SATS-WSF) was proposed. The proposed transfer stacking hybrid surrogate model was built by transferring the potential synergies of three single models to approach the numerical simulation model. Meanwhile, two infill sampling strategies, namely promising and uncertainty samples were applied to accelerate the convergence of the SATS-WSF

method and diversity of the final optimal solutions, respectively. The experimental results for single and multiple well cases confirmed that the SATS-WSF method accurately and effectively achieved integrated optimization of horizontal well spacing and hydraulic fracture stage placement in naturally fractured shale gas reservoir than other conventional methods. The specific conclusions are listed below:

- (1) The final optimal solutions of the proposed SATS-WSF method matched well with that of the NS-WSF method while reducing the computational burden of the expensive numerical simulation runs in both cases.
- (2) Due to the transfer stacking technique and infill sampling strategy, the hybrid surrogate model in the SATS-WSF method made full use of the potential synergies of the three single models,

Table 8

Values of design variables in typical steps for maximum NPV (type 1).

Optimization variables	Vales in step 1	Vales in step 25	Vales in step 50	Vales in step 75	Vales in step 100
Fracture space (m)	40.53	43.32	34.39	39.43	44.79
Fracture half-length (m)	39.42	42.76	55.65	46.61	49.38
Well length (m)	614.54	776.81	872.64	912.92	836.69
Number of fractures	15	18	25	23	19
Well space (m)	121.65	124.86	126.42	132.56	136.43

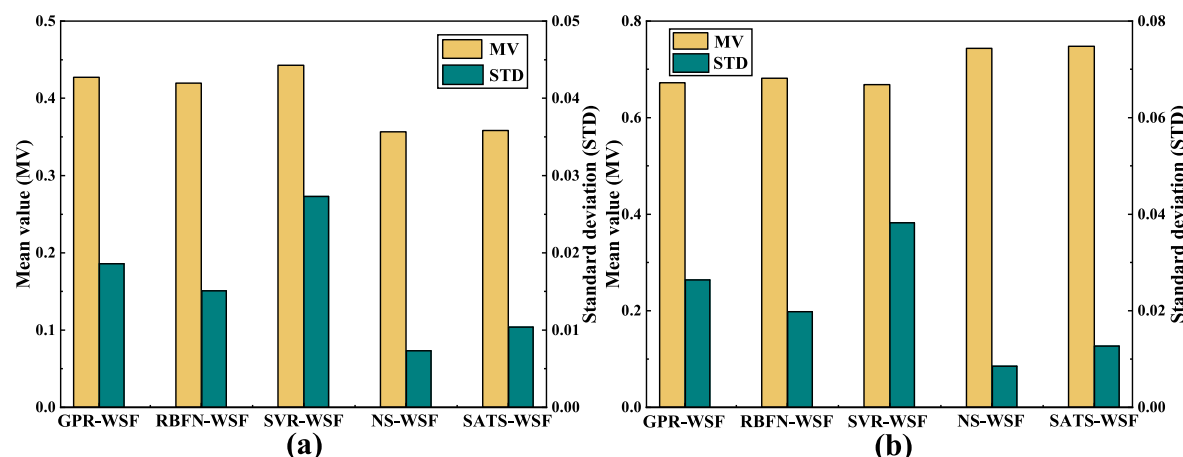


Fig. 14. The MV and STD of RHD (a) and OS (b) obtained by the five methods for type 1 with twenty runs.

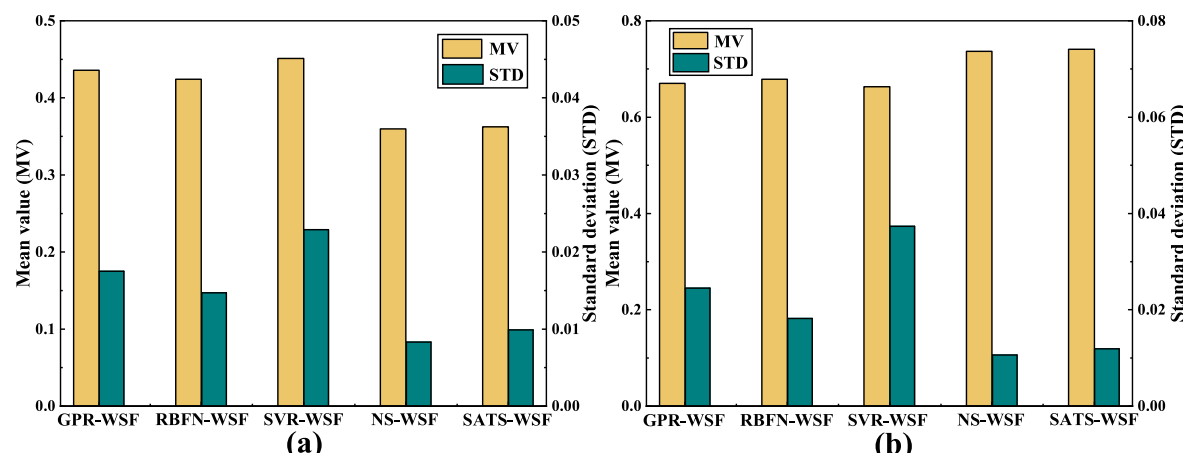


Fig. 15. The MV and STD of RHD (a) and OS (b) obtained by the five methods for type 2 with twenty runs.

Table 9

Values of design variables in typical steps for maximum CGP (type 1).

Optimization variables	Vales in step 1	Vales in step 25	Vales in step 50	Vales in step 75	Vales in step 100
Fracture space (m)	53.93	47.42	40.96	38.26	37.23
Fracture half-length (m)	46.76	48.98	53.52	58.63	62.61
Well length (m)	990.74	1025.78	1146.52	1082.23	1093.47
Number of fractures	19	22	27	29	30
Well space (m)	117.72	124.86	123.56	134.53	144.24

Table 10

Values of design variables in typical steps for maximum NPV (type 2).

Optimization variables	Vales in step 1	Vales in step 25	Vales in step 50	Vales in step 75	Vales in step 100
Fracture space (m)	43.95	40.84	36.69	39.89	45.73
Fracture half-length (m)	68.97	62.39	51.41	57.43	59.75
Well length (m)	735.29	834.68	923.56	907.58	851.72
Number of fractures	17	21	25	23	19
Well space (m)	109.74	121.92	119.21	99.64	95.42

Table 11

Values of design variables in typical steps for maximum CGP (type 2).

Optimization variables	Vales in step 1	Vales in step 25	Vales in step 50	Vales in step 75	Vales in step 100
Fracture space (m)	54.53	47.76	42.87	36.46	35.48
Fracture half-length (m)	62.24	57.53	54.75	61.45	66.86
Well length (m)	953.01	1126.48	1083.75	977.96	1058.92
Number of fractures	18	24	26	27	30
Well space (m)	113.94	133.63	125.62	132.73	126.87

which had better reliability and robustness on this shale gas horizontal well spacing and fracture stage placement optimization problem.

- (3) The alternating fracture type had better economic benefits and more gas production than the aligning fracture type. Therefore, the alternating fracture type was more suitable for shale gas “well factory” development.

The above discussions have indicated the superior performance of the established SATS-WSF method in solving integrated horizontal well spacing and hydraulic fracture stage placement in naturally fractured shale gas reservoir. Nevertheless, there are some expectations that need to be addressed in future researches. Firstly, the SATS-WSF method will be applied to solve integrated horizontal well spacing and fracture stage placement optimization design with more than two objectives. Besides, the SATS-WSF method can also be extended to solve robust optimization

with uncertainty of the geological, fracture and economic parameters such as porosity, permeability, distribution of natural fractures, fracture characteristics, cost of drilling and fracturing, and gas price. Finally, the SATS-WSF method can be used as a reference to solve similar computational expensive problems in petroleum engineering such as numerical simulation-based fracture parameters inversion and production history matching of unconventional resources.

Author contributions

Lian Wang: Conceptualization, Methodology, Investigation and Writing Original Draft.

Yuedong Yao: Writing - Review & Editing, Supervision.

Wenzhi Wang: Review & Editing.

Casper Daniel Adenutsi: Data analysis, Review & Editing.

Guoxiang Zhao: Formal analysis, Software.

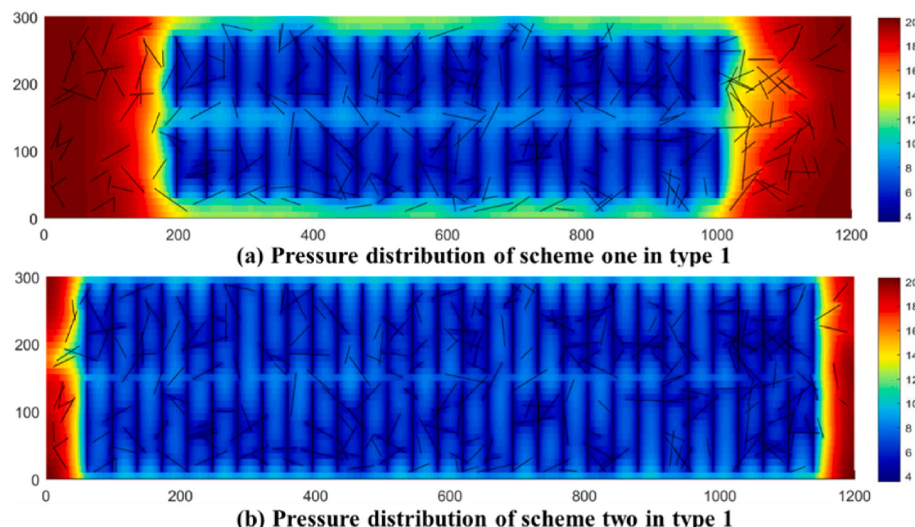


Fig. 16. Pressure distribution after 10 years' production in type 1 (MPa).

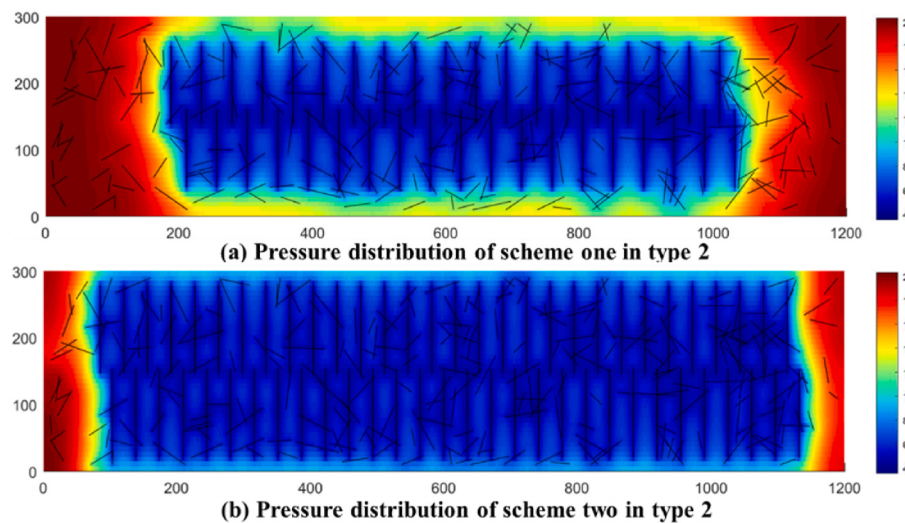


Fig. 17. Pressure distribution after 10 years' production in type 2 (MPa).

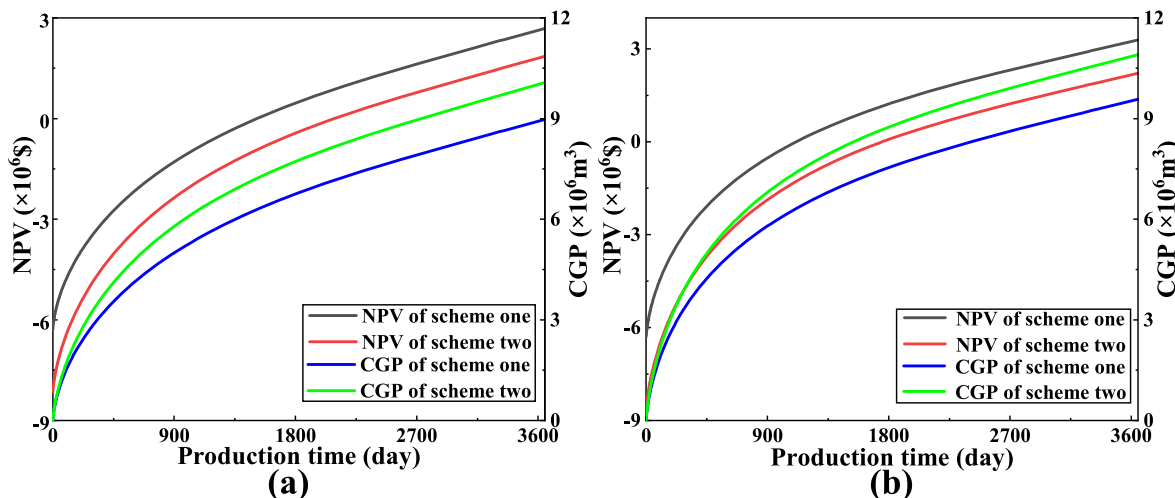


Fig. 18. NPV and CGP curves of the two schemes in type 1 (a) and type 2 (b).

Fengpeng Lai: Writing - Review & Editing, Data Curation.

Declaration of competing interest

The authors declare that they have no known competing financial interests or personal relationships that could have appeared to influence the work reported in this paper.

Acknowledgement

The authors would like to acknowledge financial support from the National Basic Research Program of China (2015CB250900) and the SINTEF for the MATLAB Reservoir Simulation Toolbox.

References

- Aanonsen, S.I., Tveit, S., Alerini, M., 2019. Using bayesian model probability for ranking different prior scenarios in reservoir history matching[J]. SPE J. 24 (4), 1490–1507.
- Baiocco, J.S., Jacob, B.P., Mazadiego, L.F., 2019. In: Uncertainty Analysis in the Multi-Objective Optimization of Hydraulic Fracture[C]//International Conference on Offshore Mechanics and Arctic Engineering. American Society of Mechanical Engineers, 58875. V008T11A050.
- Berawala, D.S., Andersen, P.O., 2019. Controlling parameters during continuum flow in shale-gas production: a fracture/matrix-modeling approach[J]. SPE J. 24 (3), 1378–1394.
- Cao, P., Liu, J., Leong, Y.K., 2016. A fully coupled multiscale shale deformation-gas transport model for the evaluation of shale gas extraction[J]. Fuel 178, 103–117.
- Chen, G., Zhang, K., Zhang, L., et al., 2020. Global and local surrogate-model-assisted differential evolution for waterflooding production optimization[J]. SPE J. 25 (1), 105–118.
- Clarkson, C.R., Nobakht, M., Kaviani, D., et al., 2012. Production analysis of tight-gas and shale-gas reservoirs using the dynamic-slippage concept[J]. SPE J. 17 (1), 230–242.
- Deb, K., Pratap, A., Agarwal, S., Meyarivan, T.A.M.T., 2002. A fast and elitist multiobjective genetic algorithm: NSGA-II. IEEE Trans. Evol. Comput. 6 (2), 182–197.
- Desbordes, J.K., Zhang, K., Xue, X., et al., 2022. Dynamic production optimization based on transfer learning algorithms[J]. J. Petrol. Sci. Eng. 208, 109278.
- Ding, S., Lu, R., Xi, Y., et al., 2020. Efficient well placement optimization coupling hybrid objective function with particle swarm optimization algorithm[J]. Appl. Soft Comput. 95, 106511.
- Drucker, H., Burges, C.J., Kaufman, L., et al., 1996. Support vector regression machines. Adv. Neural Inf. Process. Syst. 9.
- Feng, D., Bakhshian, S., Wu, K., et al., 2021. Wettability effects on phase behavior and interfacial tension in shale nanopores [J]. Fuel 290, 119983.
- Feng, D., Li, X., Wang, X., et al., 2018. Water adsorption and its impact on the pore structure characteristics of shale clay[J]. Appl. Clay Sci. 155, 126–138.
- Guo, Z., Reynolds, A.C., 2018. Robust life-cycle production optimization with a support-vector-regression proxy. SPE J. 23 (6), 2409–2427.
- He, X., Zhu, W., Santoso, R., et al., 2021. In: Fracture Permeability Estimation under Complex Physics: A Data-Driven Model Using Machine Learning[C]//SPE Annual Technical Conference and Exhibition. OnePetro.
- IEA, Paris, 2020. Global Energy Review 2020. IEA. <https://www.iea.org/reports/global-energy-review-2020>.

- Jahandideh, A., Jafarpour, B., 2016. Optimization of hydraulic fracturing design under spatially variable shale fracability[J]. *J. Petrol. Sci. Eng.* 138, 174–188.
- Jin, Z.L., Liu, Y., Durlofsky, L.J., 2020. Deep-learning-based surrogate model for reservoir simulation with time-varying well controls[J]. *J. Petrol. Sci. Eng.* 192, 107273.
- Kim, J., Lee, K., Choe, J., 2021. Efficient and robust optimization for well patterns using a PSO algorithm with a CNN-based proxy model[J]. *J. Petrol. Sci. Eng.*, 109088.
- Lie, K.-A., 2019. An Introduction to Reservoir Simulation Using MATLAB/GNU Octave: User Guide for the MATLAB Reservoir Simulation Toolbox (MRST). Cambridge University Press.
- Lin, R., Ren, L., Zhao, J., et al., 2017. Cluster spacing optimization of multi-stage fracturing in horizontal shale gas wells based on stimulated reservoir volume evaluation[J]. *Arabian J. Geosci.* 10 (2), 38.
- Moradi, D.M., Jamaliyahmady, M., 2018. The performance evaluation and design optimisation of multiple fractured horizontal wells in tight reservoirs[J]. *J. Nat. Gas Sci. Eng.* 49, 19–31.
- Omar, A., Addassi, M., Vahrenkamp, V., et al., 2021. Co-optimization of CO₂ storage and enhanced gas recovery using carbonated water and supercritical CO₂[J]. *Energies* 14 (22), 7495.
- Unpraseuth, S.T., 2008. Gaussian processes for machine learning. *J. Am. Stat. Assoc.* 103 (481), 429, 429.
- Pan, S.J., Yang, Q., 2009. A survey on transfer learning[J]. *IEEE Trans. Knowl. Data Eng.* 22 (10), 1345–1359.
- Pardoe, D., Stone, P., 2010. Boosting for regression transfer. In: Proceedings of the 27th International Conference on International Conference on Machine Learning. Omnipress, pp. 863–870.
- Plaksina, T., Gildin, E., 2017. Rigorous integrated evolutionary workflow for optimal exploitation of unconventional gas assets[J]. *Int. J. Energy Optim. Eng.* 6 (1), 101–122.
- Podhoretz, S.B., Valkó, P.P., 2014. In: Hydraulic Fracture Design for the Lower Tertiary Gulf of Mexico: Optimization under Uncertainty[C]//Offshore Technology Conference. OnePetro.
- Pouladi, B., Keshavarz, S., Sharifi, M., et al., 2017. A robust proxy for production well placement optimization problems[J]. *Fuel* 206, 467–481.
- Rahmanifard, H., Plaksina, T., 2018. Application of fast analytical approach and AI optimization techniques to hydraulic fracture stage placement in shale gas reservoirs [J]. *J. Nat. Gas Sci. Eng.* 52, 367–378.
- Santoso, R., Hoteit, H., Vahrenkamp, V., 2019. Optimization of Energy Recovery from Geothermal Reservoirs Undergoing Re-injection: Conceptual Application in Saudi Arabia[C]//SPE Middle East Oil and Gas Show and Conference. OnePetro.
- Santoso, R., He, X., Alsinan, M., et al., 2021. Uncertainty Quantification and Optimization of Deep Learning for Fracture Recognition[C]//SPE Middle East Oil & Gas Show and Conference. OnePetro.
- Sherratt, J., Haddad, A.S., Wejzerowski, F., et al., 2021. Optimising well orientation in hydraulic fracturing of naturally fractured shale gas formations[J]. *J. Nat. Gas Sci. Eng.* 94, 104141.
- Tian, J., Tan, Y., Zeng, J., et al., 2018. Multiobjective infill criterion driven Gaussian process-assisted particle swarm optimization of high-dimensional expensive problems[J]. *IEEE Trans. Evol. Comput.* 23 (3), 459–472.
- Wang, B., 2020. MRST-shale: an Open-Source Framework for Generic Numerical Modeling of Unconventional Shale and Tight Gas Reservoirs[J]. Preprints.
- Wang, L., Yao, Y., Zhang, T., et al., 2022. A novel self-adaptive multi-fidelity surrogate-assisted multi-objective evolutionary algorithm for simulation-based production optimization[J]. *J. Petrol. Sci. Eng.*, 110111.
- Wang, L., Yao, Y., Wang, K., et al., 2021. A novel surrogate-assisted multi-objective optimization method for well control parameters based on tri-training[J]. *Nat. Resour. Res.* 30 (6), 4825–4841.
- Wang, L., Li, Z.P., Adenutsi, C.D., et al., 2020. A novel multi-objective optimization method for well control parameters based on PSO-LSSVR proxy model and NSGA-II algorithm[J]. *J. Petrol. Sci. Eng.* 196, 107694.
- Waters, G.A., Dean, B.K., Downie, R.C., et al., 2009. In: Simultaneous Hydraulic Fracturing of Adjacent Horizontal Wells in the Woodford Shale[C]//SPE Hydraulic Fracturing Technology Conference. OnePetro.
- Xu, S., Feng, Q., Wang, S., et al., 2018. Optimization of multistage fractured horizontal well in tight oil based on embedded discrete fracture model[J]. *Comput. Chem. Eng.* 117, 291–308.
- Yao, J., Li, Z., Liu, L., et al., 2021. Optimization of fracturing parameters by modified variable-length particle-swarm optimization in shale-gas reservoir[J]. *SPE J.* 26 (2), 1032–1049.
- Yu, W., Sepehrnoori, K., 2013. In: Optimization of Multiple Hydraulically Fractured Horizontal Wells in Unconventional Gas reservoirs[C]//SPE Production and Operations Symposium. OnePetro.
- Zhang, H., Sheng, J., 2020. Optimization of horizontal well fracturing in shale gas reservoir based on stimulated reservoir volume[J]. *J. Petrol. Sci. Eng.* 190, 107059.
- Zhang, H., Sheng, J.J., 2021. Surrogate-assisted multiobjective optimization of a hydraulically fractured well in a naturally fractured shale reservoir with geological uncertainty[J]. *SPE J.* 1–22.
- Zhang, K., Wang, Z., Chen, G., et al., 2022. Training effective deep reinforcement learning agents for real-time life-cycle production optimization[J]. *J. Petrol. Sci. Eng.* 208, 109766.
- Zhang, L., Li, Z., Lai, F., et al., 2019. Integrated optimization design for horizontal well placement and fracturing in tight oil reservoirs. *J. Pet. Sci. Eng.* 178, 82–96.
- Zhang, T., Javadpour, F., Yin, Y., et al., 2020. Upscaling water flow in composite nanoporous shale matrix using lattice Boltzmann method[J]. *Water Resour. Res.* 56 (4), e2019WR026007.
- Zhang, T., Javadpour, F., Li, J., et al., 2021. Pore-scale perspective of gas/water two-phase flow in shale[J]. *SPE J.* 26 (2), 828–846.
- Zhong, C., Zhang, K., Xue, X., et al., 2022. Surrogate-reformulation-assisted multitasking knowledge transfer for production optimization[J]. *J. Petrol. Sci. Eng.* 208, 109486.